21. C. P. Bean and J. D. Livingston, *J. Appl. Phys.* **30**, 120s (1959).
22. B. D. Cullity, *Introduction to Magnetic Materials* (Addison-Wesley, Reading, MA, 1972), pp. 201 and 383–441.
23. J. K. Vassiliou, V. Mehrotra, M. W. Russell, E. P. Giannelis, *Mater. Res. Soc. Symp. Proc.* **206**, 561 (1991). If we take 58 K as the blocking temperature and assume that the particles are spherical with an average diameter of 85 Å, we calculate a magnetic anisotropy of 6.2×10^5 erg/cm^3. The critical radius for superparamagnetic γ-Fe_2O_3 particles at room temperature is 385 Å, corresponding to a magnetic anisotropy of 0.04×10^5 erg/cm^3. The large deviation from the value calculated for the 85 Å particles is probably due to the surface anisotropy resulting from the small particle size and possibly the presence of some Fe^{2+} ions in the structure of the oxide. Similar arguments have been used to explain the difference in magnetic anisotropy (three orders of magnitude) calculated from blocking temperature data for 100 Å NiO particles.
24. E. Kneller, in *Magnetism and Metallurgy*, A. E. Berkowitz and E. Kneller, Eds. (Academic Press, New York, 1969), vol. 1, chap. 8.
25. A. F. Jenkins and H. White, *Fundamentals of Optics* (McGraw-Hill, New York, ed. 4, 1976), p. 84.
26. W. C. McCrone and J. G. Delly, *The Particle Atlas* (Ann Arbor Science, Ann Arbor, MI, ed. 2, 1973), vol. 1, p. 72.
27. H. Takei and S. Chiba, *J. Phy. Soc. Jpn.* **21**, 1255 (1966).
28. G. V. Samaonov, Ed., *The Oxide Handbook* (Plenum, New York, 1973), p. 334. The complete optical characterization of this film is in progress.
29. This value was derived from the iron oxide weight loading, assuming a density of 5.07 g/cm^3 for γ-Fe_2O_3 and 1.0 g/cm^3 for the polymer.
30. C. J. Tauc, in *Progress in Semiconductors*, A. F. Gibson and R. E. Burgess, Eds. (Temple Press, London, 1965), vol. 9.
31. B. N. Ganguly, *Proc. IEEE Indust. Appl. Soc.* (Annual meeting, 1 to 5 October 1978, Toronto, Ontario, Canada), p. 251
32. D. K. Smith and C. Mailhiot, *Rev. Mod. Phys.* **62**, 173 (1990).
33. U. Merkt and Ch. Sikorski, *Semicond. Sci. Technol.* **5**, S182 (1990).
34. G. W. Bryant, *Phys. Rev. Lett.* **59**, 1140 (1987).
35. R. F. Ziolo *et al.*, in preparation.
36. R. Wolfe, A. J. Kurtzig, R. C. LeCraw, *J. Appl. Phys.* **41**, 1218 (1970).
37. P. Day, *Acc. Chem. Res.* **12**, 236 (1979).
38. G. B. Scott, D. E. Lacklison, J. L. Page, *Phys. Rev. B.* **10**, 971 (1974).
39. The Faraday and magnetic circular dichroism spectra of the γ-Fe_2O_3 nanocomposite have been measured in the visible and near-ultraviolet (R. F. Ziolo *et al.*, in preparation).
40. The Cornell University contribution was sponsored in part by the National Science Foundation (DMR-88188558) through the Materials Science Center. E.P.G. and B.A.W. acknowledge grants from Xerox Webster Research Center. We thank R. J. Gruber for support and encouragement. M.W.R. was supported under an IBM Fellowship administered through the Cornell Ceramics Program. We thank H. Takei and S. Chiba for supplying the reference sample of γ-Fe_2O_3. We thank R. D. Shull and R. D. McMichael (low-temperature magnetization data), R. G. Fernquist (γ-Fe_2O_3 thickness measurement), T. P. Debies (x-ray photoelectron spectroscopy), A. Orzechowski (optical microscopy), K. Kemp (scanning electron microscopy), J. A. Czerniawski (TEM), K. Johnson (TEM), R. H. Herber (Mössbauer spectroscopy), W. H. H. Günther, F. J. DiSalvo, J. W. Otto, and J. K. Vassiliou for their contributions. The Cornell High Energy Synchrotron Source facility is supported by a grant from the National Science Foundation.

23 April 1992; accepted 14 May 1992

The Chemistry of Bulk Hydrogen: Reaction of Hydrogen Embedded in Nickel with Adsorbed CH_3

A. D. Johnson, S. P. Daley, A. L. Utz, S. T. Ceyer*

Studies in heterogeneous catalysis have long speculated on or have provided indirect evidence for the role of hydrogen embedded in the catalyst bulk as a primary reactant. This report describes experiments carried out under single-collision conditions that document the distinctive reactivity of hydrogen embedded in the bulk of the metal catalyst. Specifically, the bulk H atom is shown to be the reactive species in the hydrogenation of CH_3 adsorbed on Ni(111) to form CH_4, while the H atoms bound to the surface were unreactive. These results unambiguously demonstrate the importance of bulk species to heterogeneous catalytic chemistry.

Forty years ago, several studies (*1–3*) noted a correlation between the hydrogenation activity of a Raney nickel catalyst and the hydrogen content in the catalyst, but the exact role of the hydrogen, whether it be a reactant or a modifier of the electronic structure and hence of the activity of the nickel, remains unclear (*4–6*). The reason for the dearth of information about these practically and commercially important hydrogenation reactions is the inability to carry them out under single-collision conditions, such as afforded by ultrahigh vacuum (UHV) surface science techniques, where microscopic reaction steps are discernable. Specifically, it is the inability to produce the bulk hydrogen at low H_2 pressures ($<10^{-4}$ torr) that precludes these reactions from being studied. The kinetic limitations imposed by high barriers (*7*) to dissociative absorption of H_2 into nickel metal and into many other transition metal catalysts necessitate high hydrogen pressures. However, we have recently demonstrated two methods of synthesizing bulk hydrogen in Ni under low-pressure UHV conditions (*8, 9*) and a method to detect it spectroscopically (*9*). In this report, we document the chemistry of this bulk hydrogen. We find that a bulk H atom has a reactivity that is distinct from that of a H atom adsorbed on a surface. In particular, a bulk H atom is the reactive species in the hydrogenation of CH_3 adsorbed on Ni(111) to form methane. Hydrogen atoms bound to the surface are unreactive with the CH_3 species. Analogous results are obtained for the D isotope as a bulk or an adsorbed species.

The experiment is carried out in a UHV chamber that is equipped for surface analysis and is precisely coupled to a supersonic molecular beam source. The experimental procedures are similar to our previous studies (*10–12*). In the experiment described here, bulk D is synthesized by exposure of the Ni(111) crystal at 130 K to atomic D as described previously (*8, 9*). The bulk D is characterized by a vibrational mode at 575 cm^{-1}, as measured by high-resolution electron energy loss spectroscopy (HREELS), and recombines and desorbs as D_2 between 180 and 220 K. Exposure to atomic D not only results in D embedded within the Ni lattice but also in a monolayer (ML) of deuterium adsorbed on the surface. The surface-bound D is a problem because it blocks sites necessary for the second reactant, adsorbed CH_3, that we synthesize by the dissociative chemisorption of CH_4 (*13*). Therefore, the D adsorbed on the surface must be removed. The removal of the surface-bound deuterium cannot be effected thermally because it is more stable than bulk D, recombining and desorbing between 320 and 390 K. Therefore, a nonthermal mechanism for removal of the surface-bound D is necessary.

We have recently observed such a mechanism, collision-induced recombinative desorption (*14*). In this process, a beam of energetic Xe atoms impinges on the deuterium-covered Ni(111) surface at glancing incident angles. The impacts of the collisions momentarily jostle the lattice, causing the adsorbed D atoms to recombine and desorb as D_2. We used this technique in our synthesis to sweep the deuterium off the surface, leaving the deuterium in the bulk unperturbed. Its efficacy for the H isotope is demonstrated by the HREEL spectra in Fig. 1. Figure 1A shows the vibrational spectrum of the Ni(111) crystal saturated with the H isotope so that the equivalent coverage of H in the bulk is 1.5 ML and the surface coverage is 1 ML. The symmetric and antisymmetric vibrational stretch modes for the surface-bound H are visible at 1170 and 955 cm^{-1}, respectively, and the threefold degenerate vibrational mode for H bound in an octahedral interstitial site is visible at 790 cm^{-1} (*9*). After exposure to 9×10^{17} Xe atoms incident at 40° from the normal angle with 144 kcal mol^{-1} of energy (Fig. 1B), the surface mode at 1170 cm^{-1} is

Department of Chemistry, Massachusetts Institute of Technology, Cambridge, MA 02139.

*To whom correspondence should be addressed.

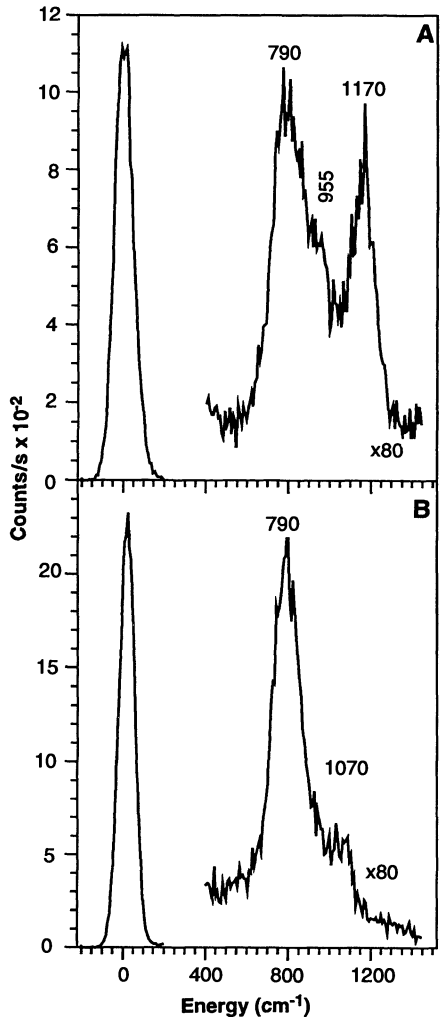

Fig. 1. (**A**) An HREEL spectrum of a Ni(111) crystal at 80 K containing 1.5 ML of H in the bulk and covered with 1 ML of H on the surface. The spectrum is collected at 12° from the specular angle with a 5.5-eV electron impact energy. The loss features at 1170 and 955 cm^{-1} are the symmetric and antisymmetric modes of the surface bound hydrogen, respectively, and the feature at 790 cm^{-1} is the bulk H mode. (**B**) After exposure to 9 × 10^{17} Xe atoms incident at 40° from the normal angle with 144 kcal mol^{-1} of energy. The electron impact energy is 5 eV.

no longer present while the bulk mode is unperturbed. The small shoulder at 1070 cm^{-1} is the symmetric stretch of surface-bound H at a coverage that is estimated from the value of the frequency and the intensity of the mode to be less than 0.05 ML. These results show that collision-induced recombinative desorption removed 95% of the surface-bound H. A similar efficiency was observed for removal of the surface-bound D isotope.

Having removed the surface D, the crystal at 80 K was then exposed to a beam of CH_4 incident at the normal angle and with 17 kcal mol^{-1} of energy. The high translational energy is necessary to overcome the barrier to dissociative chemisorption to form an adsorbed CH_3 species and an adsorbed H atom (*13*). The resulting vibrational spectrum measured after depositing 0.15 ML of CH_3 on the surface of the Ni crystal containing an equivalent of 1.1 ML of deuterium in the bulk is shown in Fig. 2. The symmetric and antisymmetric CH_3 deformation modes are observed at 1225 and 1320 cm^{-1}, respectively, and the C–H stretching modes appear unresolved in this spectrum at 2675 cm^{-1} as assigned previously (*15*). The intense mode at 575 cm^{-1} is the bulk deuterium vibrational mode, whereas the mode at 810 cm^{-1} is assigned to residual surface deuterium.

With the reactants now synthesized, the crystal with 2 ML of bulk deuterium was heated at a rate of 2 K s^{-1} and the partial pressures at masses 4, 15, 16, 17, 18, 19, and 20 were monitored simultaneously by a quadrupole mass spectrometer. The resulting thermal desorption spectra are shown in Fig. 3. At the temperature at which the bulk deuterium makes its way out onto the surface and desorbs, 180 K, there is rapid desorption of only one product, CH_3D, at mass 17. The signal at masses 16 and 15 arises from the cracking of CH_3D in the electron bombardment ionizer of the quadrupole mass spectrometer. The observed ratio of the peak signal at masses 17:16:15 is 1:0.74 ± 0.04:0.25 ± 0.04, whereas the expected ratio is 1:0.77:0.21 (*16*). The uncertainties represent 95% confidence limits on at least 15 measurements. No signal is observed at masses 19 and 20. The signal at mass 18 is 3 ± 1% of the signal at mass 17 and arises from the natural abundance of ^{13}C. The very weak signal at masses 16 and 15 between 230 and 280 K originates from desorption of CH_4 that was physisorbed on some part of the crystal cryostat. It is also visible in a thermal desorption spectrum measured under identical reaction conditions except for the use of a very low incident energy for CH_4 (1 kcal mol^{-1}), which precludes the formation of the adsorbed CH_3 reactant. An Auger spectrum, measured after ramping the crystal to 200 K, just beyond the desorption temperature of CH_3D, shows that all of the 0.15 ML of carbon has been removed by the formation of CH_3D. This observation is additional corroboration that the mass 16 signal between 230 and 280 K does not originate from the Ni surface.

In order to confirm the distinctive reactivity of the bulk D or H atom towards methane formation, similar experiments

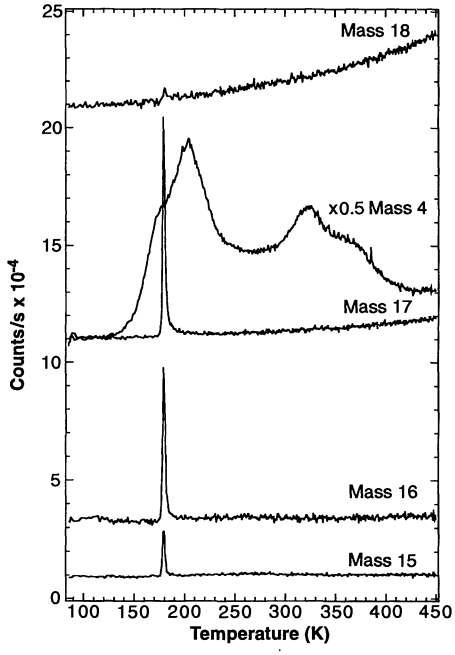

Fig. 3. Partial pressure at masses 4, 15, 16, 17, and 18 as a function of crystal temperature for a heating rate of 2 K s^{-1} from a crystal containing 2 ML of D in the bulk and 0.15 ML of CH_3 and 0.15 ML of H on the surface.

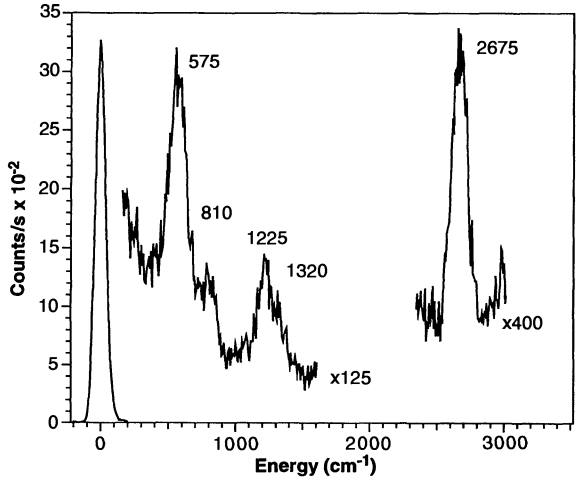

Fig. 2. An HREEL spectrum collected at 12° from the specular angle with an electron impact energy of 4.2 eV from a crystal at 80 K containing 1.1 ML of D in the bulk and covered with 0.15 ML of CH_3 and 0.15 ML of H on the surface. The CH_3 is produced from the translational activation of CH_4 incident at 17 kcal mol^{-1}.

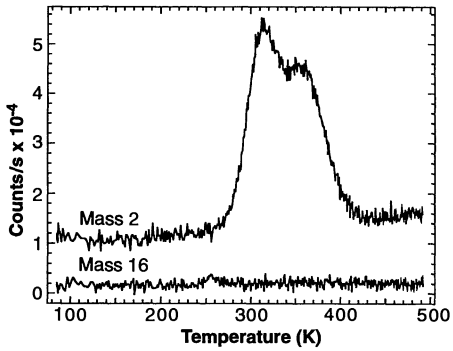

Fig. 4. Partial pressure at masses 2 and 16 as a function of crystal temperature for a heating rate of 2 K s^{-1} from a crystal covered with about 0.85 ML of surface-bound H and 0.15 ML of CH_3.

were carried out in the absence of bulk D or H but in the presence of surface-bound D or H. Adsorbed methyl radicals are produced by the dissociative chemisorption of 17 kcal mol^{-1} CH_4 on a clean surface. The surface was then exposed to molecular deuterium or hydrogen, which resulted in approximately 0.85 ML of adsorbed D or H atoms. The crystal temperature is then ramped at 2 K s^{-1}. The resulting thermal desorption experiment for the case of surface-bound H isotope is shown in Fig. 4. No methane was observed to desorb at any temperature. The hydrogen bound to the surface as well as the hydrogen produced from the decomposition of CH_3 recombines and desorbs between 300 and 400 K. Carbon is observed by Auger spectroscopy to remain on the surface after heating to 500 K.

Mono-deuterated methane was formed solely by the reaction with bulk deuterium. The surface-bound D was unreactive with CH_3. The reaction likely proceeds by the direct recombination of a bulk D atom with CH_3 because the interstitial octahedral site in which the D atom is bound (*14*) is directly beneath the threefold hollow surface site on which the CH_3 species is bound (*15*). As the surface temperature is raised, the absorbed D atom moves up toward the surface where it encounters the CH_3 species. Because the D atom has the correct orientation required by the transition state for sp^3 hybridization, it reacts with CH_3, immediately desorbing as CH_3D. The reaction of CH_3 with a surface-bound D atom probably does not occur because access of the D atom to the Ni_3–C bond is blocked (*17*).

This result documents a new mechanism for a surface reaction, a reaction between an adsorbed and an absorbed species, and it unambiguously demonstrates the importance of bulk species as reactants in heterogeneous catalytic chemistry. This mechanism may be operable in many catalytic hydrogenation reactions.

REFERENCES AND NOTES

1. H. A. Smith, A. J. Chadwell, Jr., S. S. Kirslis, *J. Phys. Chem.* **59**, 820 (1955).
2. R. J. Kokes and P. H. Emmett, *J. Am. Chem. Soc.* **81**, 5032 (1959).
3. ———, *ibid.* **82**, 4497 (1959).
4. P. Gajardo, M. C. Lartiga, S. C. Droguett, *J. Phys. Chem.* **82**, 2323 (1978).
5. I. Nakabayashi, T. Hisano, T. Terazawa, *J. Catal.* **58**, 74 (1979).
6. M. Matsuyama *et al.*, *ibid.* **102**, 309 (1986).
7. G. Alefeld and J. Völkl, Eds., *Hydrogen in Metals I & II* (Springer-Verlag, Berlin, 1986).
8. K. J. Maynard *et al.*, *Faraday Discuss. Chem. Soc.* **91**, 437 (1991).
9. A. D. Johnson, K. J. Maynard, S. P. Daley, Q. Y. Yang, S. T. Ceyer, *Phys. Rev. Lett.* **67**, 927 (1991).
10. J. D. Beckerle, A. D. Johnson, Q. Y. Yang, S. T. Ceyer, *J. Chem. Phys.* **91**, 5756 (1986).
11. J. D. Beckerle *et al.*, *ibid.* **93**, 4047 (1990).
12. S. T. Ceyer, *Science* **249**, 133 (1990).
13. M. B. Lee, Q. Y. Yang, S. T. Ceyer, *J. Chem. Phys.* **87**, 2724 (1987).
14. A. D. Johnson, thesis, Massachusetts Institute of Technology, Cambridge (1991).
15. S. T. Ceyer, *Langmuir* **6**, 82 (1990).
16. A. Cornu and R. Massot, *Compilation of Mass Spectral Data* (Heyden, France, 1966).
17. H. Wang and J. L. Whitten, *J. Chem. Phys.* **96**, 5529 (1992).

18. Supported by the Department of Energy, Basic Energy Sciences (DE-FG02-89ER14035) and the Petroleum Research Fund (24882-AC5).

1 April 1992; accepted 20 May 1992

Phototaxis of Spiral Waves

Mario Markus,* Zsuzsanna Nagy-Ungvarai,† Benno Hess

The drift of spiral waves toward regions of higher light intensity was observed experimentally in the ruthenium-catalyzed Belousov-Zhabotinsky reaction. A light gradient can thus be used to manipulate optical information in new computational systems based on photochemical media. The drift of a gradient that is rotationally invariant in space is three to four times as fast as that of a translationally invariant gradient. Simulations based on the use of a cellular automaton, which is made isotropic by a semirandom distribution of cells, are in agreement with the experimental results.

Spiral waves, rotating without a pacemaker and without attenuation, have been observed in different areas of science and in a variety of excitable media [for reviews, see (*1*)]. An area in an excitable medium may become excited by a suprathreshold perturbation; after excitation this area becomes refractory, slowly returning to the receptive state, where it can be excited again. Spiral waves in each of these media have several geometric and dynamic properties in common. Examples include heart muscle (*2–4*), the slime mold *Dyctiostelium discoideum* (*5*), the retina (*6*), and the Belousov-Zhabotinsky (BZ) reaction (*7, 8*).

The BZ reaction, when catalyzed by the ruthenium bipyridyl complex, $Ru(bpy)_3^{2+}$, is sensitive to visible light (*9*). The Br^- release in the reaction between BrO_3^- and the excited $Ru(bpy)_3^{2+}$ complex decreases the rate of autocatalysis, which is directly related to the velocity of wave propagation (*7*). In this context, it has been proposed that excitable media can be used in the implementation of new computational systems, such as associative memory devices (*10*) and learning machines (*11*). Searching for possibilities to manipulate spiral waves in such systems, researchers have shown experimentally that, if light intensity varies in time with a period equal to that of the waves, these are linearly displaced ("resonance drift") (*12*). Brazhnik *et al.* (*13*) have theorized that the rotation of the spiral tip around its core in a spatial light gradient is equivalent to a periodic light modulation and thus should also lead to a spiral drift. They predicted that this drift should occur in the direction in which the critical curvature decreases, which according to our measurements corresponds to the direction of increasing light intensity. One should thus expect a "phototaxis" of the spirals. However, this idea has not been verified experimentally so far.

In our first attempts to measure this phototactic phenomenon, we encountered the difficulty of producing a constant light gradient (a linear dependence of the light intensity, I, on the spatial coordinate, x). We transmitted the visible portion of the parallel light beam of a Cermax LX300 lamp through a slide with the photograph of a computer-generated gray-level function $g(x)$ on it. A linear gray-level function $g(x)$ yielded large deviations from linearity after photographing. However, we found that a linear $I(x)$ can be obtained in our case by setting

$$g(x) = (1 - e^{-x/d})/(1 - e^{-1}),\ x \in [0,d]$$

Our experiments were performed with two types of spatial distributions of light intensity: (i) an axial gradient, where x is the

Max-Planck-Institut fur Ernährungsphysiologie, Rheinlanddamm 201, W-4600 Dortmund, Germany.

*To whom correspondence should be addressed.
†On leave from Lorand Eotvös University, Institute of Inorganic and Analytical Chemistry, Budapest, Hungary.